Functional Ecology 2005

Functional linkages between leaf traits and net photosynthetic rate: reconciling empirical and mechanistic models

B. SHIPLEY,*† D. VILE,*‡ E. GARNIER,‡ I. J. WRIGHT§ and H. POORTER¶

*Département de Biologie, Université de Sherbrooke, Sherbrooke (QC), Canada J1K 2R1, ‡Centre d'Ecologie Fonctionnelle et Evolutive (CNRS), Montpellier Cedex 1, France, §Department of Biological Sciences, Macquarie University, Sydney 2109, Australia, ¶Plant Ecophysiology, Utrecht University, PO Box 800·84, 3508 TB Utrecht, the Netherlands

Summary

1. We had two objectives: (i) to determine the generality of, and extend the applicability of, a previously reported empirical relationship between leaf-level net photosynthetic rate (A_M, nmol g^{-1} s^{-1}), specific leaf area (SLA, m^2 kg^{-1}) and leaf nitrogen mass fraction (N_M, mmol g^{-1}); and (ii) to compare these empirical results with a mechanistic model of photosynthesis in order to provide a mechanistic justification for the empirical pattern.
2. Our results were based on both literature and original data. There were a total of 160 and 87 data points for the leaf-level and whole-plant data, respectively.
3. Our multiple regression for single leaves was $\ln(A_M) = 0{\cdot}66 + 0{\cdot}71 \ln(\text{SLA}) + 0{\cdot}79 \ln(N_M)$, $r^2 = -0{\cdot}80$; only the intercept (0·11) differed for the whole-plant data. These results are not significantly different from previously published relationships.
4. We then converted the mechanistic model of Evans and Poorter, and a modified version which includes leaf lamina thickness (T) and leaf dry matter (tissue) concentration (C_M), into directed acyclic graphs. We then derived reduced graphs that involved only T, C_M, SLA, N_M and A_M. These were tested using structural equation modelling, with measured lamina thickness (T) and leaf dry matter ratio (LDMR, g dry mass g^{-1} fresh mass) as indicators of T and C_M. The original Evans–Poorter model was rejected, but the modified version fitted the structural relationships well. The same qualitative models also applied to the whole-plant data, although the path coefficients sometimes differed.
5. Using simulations, we show that the original Evans–Poorter model predicts a positive correlation between SLA and N_M that maximizes A_M. The data closely follow this predicted relationship. The correlation between the actual values of A_M (standardized units) and the predicted values obtained from the modified Evans–Poorter model was 0·74 and increased to 0·82 once three outlier points were removed.
6. These results provide a mechanistic explanation for the empirical trends relating leaf form and carbon fixation, and predict that SLA and leaf N must be quantitatively co-ordinated to maximize C fixation.

Key-words: assimilation rate, leaf nitrogen mass fraction, leaf thickness, leaf tissue concentration, leaf tissue density, LDMR, path analysis, photosynthesis, SLA, structural equation models

Functional Ecology (2005)
doi: 10.1111/j.1365-2435.2005.01008.x

Introduction

How do leaf attributes interact directly and indirectly to determine carbon fixation? If we can express such interactions in a mathematical model, then we can explore how different trade-offs between such attributes might have contributed to the evolution of leaf form and function. This is our basic goal. However, to be useful such models must be empirically testable, generally applicable and mechanistic, so that such trade-offs represent biological or physical constraints rather than statistical artefacts.

Carbon fixation is well understood at the physiological level, and this understanding can be translated into mathematical models for individual leaves (Farquhar & Von Caemmerer 1982). The variables, parameters and functions of such mechanistic models can be mapped

†Author to whom correspondence should be addressed. E-mail: Bill.Shipley@Usherbrooke.ca

directly onto the underlying physiology. Unfortunately, such models require species-specific and environment-specific parameters, which makes them unrealistic for comparative ecology.

At the other extreme are empirical regression equations that relate easily measured plant attributes to particular components of C fixation. For instance, Field & Mooney (1986) reported interspecific regressions between net photosynthetic rate (A_M) measured in the field and leaf nitrogen, as well as between A_M and specific leaf area (SLA). Further work has produced multiple regression models between the net photosynthetic rate of a leaf growing in full light and a combination of its specific leaf area and its nitrogen mass fraction (N_M, N mass per unit leaf dry mass) (Reich *et al*. 1997; Reich *et al*. 1998; Garnier *et al*. 1999; Reich *et al*. 1999; Shipley & Lechowicz 2000; Meziane & Shipley 2001). Such interspecific regression models have advantages. Being purely phenomenological, they impose no mechanistic constraints on the model and maximize empirical predictive ability. They are more general because they involve many different species measured in the field. Finally, the independent variables are relatively few and are easily measured, allowing easy extrapolation to new species.

Some of these advantages are also disadvantages. In particular, being purely phenomenological, these multiple regressions impose no constraints on the data due to hypothesized mechanistic linkages between variables. Because no hypothesized constraints are imposed, no causal assumptions can be tested. Because the causal processes that describe the generation of the data are not logically linked to the regression model, it is impossible to predict how the behaviour of the model would change if the environmental conditions of relationships between the leaf traits change.

Our objective is to combine the strengths of empirical and physiological, process-oriented models. Specifically, we use structural equation modelling and the graph theoretic operation of 'd-separation' to derive the predicted patterns of direct and indirect linkages between the same set of easily measured leaf attributes that are used in the general empirical models, given a mechanistic model of leaf gas exchange proposed by Evans & Poorter (2001). We then determine if the results, obtained from single leaves, can be extrapolated to whole plants. Finally, we explore the predictions of the mechanistic model.

The Evans–Poorter model

SLA is the ratio of the projected area (L_A) of a leaf to its dry mass (M):

$$SLA = \frac{L_A}{M}. \qquad \text{eqn 1}$$

SLA is also the inverse of the product of average lamina thickness (T) and leaf dry mass (tissue) concentration (C_M); C_M is the dry (i.e. tissue) mass per leaf volume. Specifically, since the volume (V) of a laminar leaf is $V = TL_A$, then:

$$\text{SLA} = L_A/M = (V/T)/M = V/MT = 1/T(M/V) = (1/TC_M) \qquad \text{eqn 2}$$

Evans & Poorter (2001) published a mechanistic simulation model involving SLA and leaf N_M, and other physiological attributes related to leaf gas exchange. Its purpose was to explore how changes in SLA and N partitioning affect C fixation as irradiance varies; like any model, some processes are ignored for simplicity (variation in cell-wall resistance, the tortuosity of gas diffusion paths, internal shading of chloroplasts). Although each equation in this mechanistic model was established from the biochemistry of photosynthesis and empirical data, the causal topology of the model (the assumptions of direct and indirect linkages between the variables) has not been tested empirically.

The Evans–Poorter model simulates the net rate of photosynthetic electron transport per unit leaf mass (J_M, equation 3) based on the fraction of photosynthetically active radiation (PAR) absorbed by the leaf (α), the electron transport capacity (J_{max}) and the incident PAR (I); parameters are set to those values reported for 1000 µmol photons m^{-2} s^{-1} by Evans & Poorter (2001) (Table 1).

$$J_M = \text{SLA}\left[\frac{\phi\alpha I + J_{max} - \sqrt{(\phi\alpha I + J_{max})^2 - 4\Theta\phi\alpha I J_{max}}}{2\Theta} - R_d\right] = \frac{J_A}{T \cdot C_M} \qquad \text{eqn 3}$$

In this paper a subscript M refers to a mass-based value and a subscript A refers to an area-based measure, with the exception of J_{max} which is also an area-based measure. SLA enters the model in three ways. First, α is a saturating function of chlorophyll content per unit leaf area (χ_A). χ_A is related to organic N content per unit leaf area (N_A), the fraction of organic N allocated to pigment–protein complexes (ϕ_P), and the ratio of N to chlorophyll in these pigment–protein complexes (η); the value of 76 was obtained empirically:

$$\alpha = \frac{\chi_A}{\chi_A + 76} = \frac{\frac{10^3 N_A \phi_P}{\eta}}{\frac{10^3 N_A \phi_P}{\eta} + 76} = \frac{\frac{10^3\left(\frac{10^3 N_M}{\text{SLA}}\right)\phi_P}{\eta}}{\frac{10^3\left(\frac{10^3 N_M}{\text{SLA}}\right)\phi_P}{\eta} + 76} = \frac{\frac{10^6 N_M T C_M \phi_P}{\eta}}{\frac{10^6 N_M T C_M \phi_P}{\eta} + 76} \qquad \text{eqn 4}$$

Second, J_{max} (electron transport capacity per area) is also a function of $N_A = N_M/\text{SLA}$, ϕ_P, η, the soluble

Table 1. Parameter values used in numerical simulations of the Evans–Poorter model

Parameter	Units	Value
ϕ (maximum quantum yield)	mol e^- (mol photon)$^{-1}$	0·425
Θ (curvature factor)	unitless	0·78
R_d (daytime respiration rate)	μmol e^- m^{-2} s^{-1}	8
ϕ_P (organic N fraction to pigment–protein complexes)	unitless	0·13
η (ratio of N to chlorophyll in pigment–protein complexes)	unitless	41
υ (soluble protein N per unit electron transport capacity)	mol N (mmol e^-)$^{-1}$	0·425
N_O (amount of organic N per unit area that is not soluble or in thylakoids)	mmol m^{-2}	16·5% of total
Γ^* (CO_2 photocompensation point)	μbar	36·9
p_i (internal CO_2 partial pressure)	Pa	30

protein N per unit electron transport capacity (ν) and the amount of organic N per unit area that is not soluble or in the thylakoids (N_O, 16·5% of N_A in Evans & Poorter 2001); the value of 0·079 was obtained empirically:

$$J_{max} = \frac{\frac{10^3 N_M}{SLA}\left(1 - \frac{33{\cdot}1\phi_P}{\eta}\right) - N_O}{\nu + 0{\cdot}079} = \frac{10^3 N_M T C_M\left(1 - \frac{33{\cdot}1\phi_P}{\eta}\right) - N_O}{\nu + 0{\cdot}079} \quad \text{eqn 5}$$

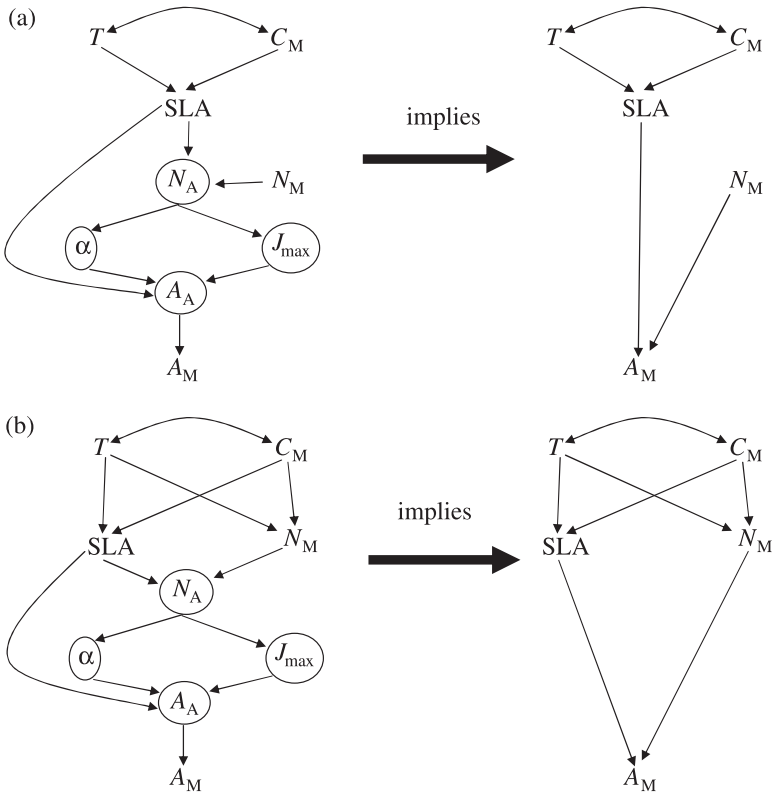

Fig. 1. (a) The Evans–Poorter model relating specific leaf area (SLA) and net photosynthetic rate per unit mass (A_M) as a directed acyclic graph (left) and the reduced graph (right) involving only the five variables in this study. (b) The modified version of the Evans–Poorter model in which leaf thickness (T) and leaf dry matter concentration (C_M) are causes of variation in leaf nitrogen content per unit dry mass (N_M). Other variables: N_A (leaf N content per unit projected area); α (proportion of incident PAR captured by the leaf); J_{max} (electron transport capacity); A_A (net leaf photosynthesis per unit leaf area).

We convert J_A to A_A, given Γ^* (CO_2 photocompensation point) and p_i (internal CO_2 partial pressure) (Von Caemmerer *et al.* 1994). Finally, J_M is equal to J_A (within square brackets in equation 3) × SLA. This mechanistic model can be shown in the form of a directed acyclic graph (Fig. 1a).

A MODIFICATION OF THE EVANS–POORTER MODEL

Although equations 3–5 can be expressed equivalently as functions of either SLA or $1/(TC_M)$, both T and C_M are indirect causes of A with respect to SLA in the original Evans–Poorter model; in fact, the original model did not decompose SLA into T and C_M. To see this, note that we can change both T and C_M in these equations without changing either α, J_{max} or J_M so long as the product (TC_M) is constant, as this is equivalent to keeping SLA constant. The only effect of SLA in the original Evans–Poorter model is to convert from mass-based to area-based values by changing the ratio of projected surface to dry mass. However, it is possible that T and C_M have effects on A_M that are independent of their effects on the surface : dry mass ratio (SLA). If this is true, then changing T and C_M, even when their product (thus SLA) is constant, will change those variables that are causally closer to A_M (α, J_{max}, A_M). If this occurs, then optimizing SLA for a given irradiance is not enough, as different leaf thicknesses (T) and leaf dry mass concentrations (C_M) could affect leaf N_M – and thus photosynthetic rate – even when their product (TC_M), thus SLA, is constant. If so, then the leaf must optimize SLA, T and C_M simultaneously, and each could have different ecological consequences in different environments.

There are several reasons to expect that T and C_M could effect photosynthesis independently of their effects on SLA. The first is purely geometrical and relates to the surface : volume ratio of a cell. Consider a mesophyll cell. Relatively high proportions of cell-wall compounds are expected in smaller cells with a high ratio of cell wall to cell volume (Poorter & Villar 1997). On the other hand, a significant proportion of organic N, between 40 and 70% in Evans & Poorter (2001), is in solution. Furthermore, the mass of N per

volume of leaf water is less variable between species than either N fraction per unit dry mass or per unit leaf area (Roderick *et al*. 1999a, 1999b). If we increase the volume of the cell, then the amount of cytoplasm (and therefore N) will increase more rapidly than the amount of cell wall (and therefore dry mass). Nitrogen content per unit cell dry mass would therefore increase while dry mass per cell volume would decrease, resulting in a negative correlation between N_M and C_M. Not all dry mass is in the cell wall, but the overall pattern appears to hold. Poorter & Villar (1997) showed that N_M was positively correlated with amounts of other cytoplasmic and vacuolar compounds, and negatively correlated with amounts of structural and non-structural carbohydrates and other cell-wall compounds. A similar correlation would exist when comparing leaves with different sizes of cells. The strength of this correlation would depend on the trade-off between cell size and number, and leaf thickness (Pyankov *et al*. 1999). Second, species with a high C_M tend to have more collenchyma and sclerenchyma cells (Garnier & Laurent 1994; Van Arendonk & Poorter 1994), which would also increase C_M while decreasing N_M. Finally, increases in non-structural carbohydrates would increase C_M while decreasing N_M by increasing cell dry mass without an increase in cell N. Based on these considerations, we propose a modification of the original Evans–Poorter model, in which T and C_M affect N_M independently of their combined effects on changing the ratio of projected leaf surface area to leaf dry mass (SLA). The directed graph of this modified model is shown in Fig. 1(b).

MANIPULATING AND TESTING CAUSAL GRAPHS

A hypothesized network of cause–effect links between variables, in the form of directed acyclic graphs such as those shown in Fig. 1, generates a multivariate probability distribution. All constraints in this distribution that are imposed by the hypothesized causal network can be obtained from the graph theoretic operation of 'd-separation' (Spirtes *et al*. 1993; Pearl 1995, 2000; Shipley 2000a; Spirtes *et al*. 2000). These constraints, which follow necessarily from the topology of the direct and indirect links that form the hypothesized causal network, can be tested statistically irrespective of the functional form or the distribution of each variable (Shipley 2000a, 2000b, 2003). If the data approximately agree with the assumptions of multivariate normality and linearity, as is the case in this paper, such tests are equivalent to the maximum likelihood test of structural equation modelling (Pearl 2000).

As many of the variables in the original Evans–Poorter model (e.g. α, χ_A, J_{max}) are not generally measured in large interspecific studies, it is possible to derive a new directed acyclic graph involving only the measured variables (SLA, T, C_M, N_M and A_M), which preserves the same causal topology between these measured variables as hypothesized in the original causal graph (Spirtes *et al*. 2000). Figure 1(a,b) shows the reduced graphs that result from the Evans–Poorter model and its modification. If any of the statistical constraints suggested by these new graphs do not agree with the empirical data, then the original ones must also be rejected. This ability to translate between causal graphs has two important consequences. First, it allows us to falsify the original cause–effect network if we can falsify the simpler one. Second, it allows us directly to map the causal paths of the original graph to those in the simpler graph and to provide a mechanistic interpretation of such simpler graphs which, when translated into equations, are closer to the simpler empirical equations.

Methods

DATA SOURCES

Table 2 summarizes the data. The measured variables were specific leaf area (SLA, $m^2\ kg^{-1}$); T' (estimated average lamina thickness, μm); leaf dry matter ratio (LDMR, mg dry mass g^{-1} fresh mass); leaf N mass per unit leaf dry mass N_M (mmol N g^{-1}); and net C assimilation rate (A_M, mg C g^{-1} day^{-1}) from species with widely differing leaf morphologies, including herbaceous and woody species, and obtained from field measurements taken in full sunlight. The leaf-level data came mainly from the literature although we also report some unpublished results; all whole-plant data are from herbaceous species grown in hydroponic culture in controlled conditions and at lower irradiances than those occurring in the field. We limited our literature search to those publications that either reported each of the above variables, or for which sufficient information was available to derive them. There were a total of 154 and 43 data points for the leaf-level and whole-plant data, respectively.

STRUCTURAL EQUATION MODELS

The measured leaf thickness for the field data was estimated in different ways by different authors, based on measurements taken at different places on the leaf blade; thus it has an error component of unknown magnitude. We therefore model true leaf thickness (T) as a latent variable and the measured leaf thickness (T') as an observed variable that is caused by the true thickness plus random errors that are independent of the other variables in the model. We fixed the path coefficient from the true thickness to this estimated value (i.e. $T' \rightarrow T$) to 1·0, which assumes no systematic bias in the measurement errors, i.e. the magnitude of the measurement error is independent of the true leaf thickness. LDMR is strongly correlated with C_M ($r = 0{\cdot}76$) (Shipley & Vu 2002). However, its error component ($1 - 0{\cdot}76^2 = 0{\cdot}42$) was substantial in that study, so we also include C_M as a latent variable whose path

Table 2. Summary of data sources

Author/s	Plant types and conditions	Number of species (number of data points)
Leaf-level measurements in field		
Abrams & Mostoller (1995)	Woody trees in drought	6 (6)
Chazdon & Kaufmann (1993)	*Piper arieianum*, *Piper sancti-felicis*	2 (2)
Kloeppel & Abrams (1995)	Species of *Acer*	3 (3)
Körner & Diemer (1987)	Woody and herbaceous monocots and dicots	21 (21)
Garnier (unpublished data)	Woody and herbaceous monocots and dicots	51 (51)
Pammenter *et al*. (1986)	*Agrostis magellanica*, *Agrostis stolonifera*	2 (2)
Witkowski *et al*. (1992)	Two species of *Banksia*	2 (4)
Woodward (1986)	*Vaccinium myrtillus*	1 (3)
Wright (2001)		61 (67)
Zotz & Winter (1996)	*Uncaria tomentosa*	1 (1)
Plant-level measurements in laboratory		
Atkin *et al*. (1996)	Grasses	6 (6)
Den Dubbelden (1994)	Herbaceous monocots and dicots	12 (12)
Dijkstra & Lambers (1989)	*Plantago major*	1 (2)
Roumet *et al*. (unpublished data)	Grasses	11 (11)
Poorter (1990)	Herbaceous monocots and dicots, 285 μmol m^{-2} s^{-1}	8 (8)
Poorter & Remkes (1990)	Herbaceous monocots and dicots	24 (24)
Van den Boogaard *et al*. (1996)	*Triticum aestivum*	1 (4)
Van der Werf *et al*. (1993)	Grasses	2 (2)
Van Rijn (2001)	Herbaceous monocots, 450 μmol m^{-2} s^{-1}	6 (6)
Van Rijn *et al*. (2000)	*Hordeum spontaneum*, 450 μmol m^{-2} s^{-1}	1 (11)

coefficient to LDMR is fixed at 1·0; again, this assumes that the strength of the correlation between LDMR and C_M does not vary systematically with C_M. All other measured variables (N_M, A_M, SLA) can be measured with accuracies of <1% of the total variation of the variables. Bias due to measurement error of these variables would be negligible and can be ignored. Shipley (2000a) provides details of fitting and interpreting latent variables. The data on whole-plant net photosynthetic rate did not report mean leaf thickness, so we have estimated it using SLA and leaf dry matter ratio (LDMR, leaf dry mass/leaf fresh mass): $T \approx 1/(\text{SLA} \times \text{LDMR})$.

Structural equation modelling assumes linearity between variables and (approximate) multivariate normality (Shipley 2000a). All variables were therefore ln-transformed before analysis in order to better approximate multivariate normality, and because these variables typically have non-linear (allometric) relationships with each other. As, by definition, $\ln(\text{SLA}) = -1 \ln(T) - 1 \ln(C_M)$, we fixed the paths linking SLA to its two components to –1.

Each path model was fitted using maximum likelihood methods, and the observed and predicted covariance matrices were compared using the maximum likelihood χ^2 statistic using the EQS program (Bentler 1995). A significant ($P < 0{\cdot}05$) value indicates a significant lack of fit between the observed and predicted values, and means that the model must be rejected; see Shipley (2000a) for more details of this test.

All other statistical analyses and simulations were conducted using SPLUS (SPLUS 1999).

Results

EMPIRICAL TRENDS

There are clear systematic relationships between leaf attributes, despite varying degrees of scatter (Fig. 2). The whole-plant measurements (filled symbols) generally fall within the cloud of points representing the measurements on single leaves. The relationship between leaf thickness and leaf dry matter concentration is more complicated. Although the slope ($P < 0{\cdot}001$) and the intercept ($P < 0{\cdot}001$) of the relationship between these two variables in the whole-plant data are different from those shown in the leaf-level data (ANCOVA), the points of the two data sets largely overlap.

We regressed $\ln(A_M)$ on ln(SLA), $\ln(N_M)$ and a dummy variable representing the type of data (leaf level or whole plant) and evaluated significance using type III sums of squares. Although the slopes with respect to both ln(SLA) and $\ln(N_M)$ were significant ($P < 0{\cdot}05$), these slopes never varied significantly between the leaf-level and whole-plant data sets ($P = 0{\cdot}09$ and 0·05, respectively) and there was no significant interaction between ln(SLA) and $\ln(N_M)$. There was, however, a significant difference between the intercepts of the two types of data ($t = -5{\cdot}28$, 193 df, $P < 0{\cdot}0005$). The resulting regression equations explained 80% of the variance in $\ln(A_M)$ with a residual standard error (SE) of 0·43. The equations (± SE) were:

$$\text{leaves} = \ln(A_M) = 0{\cdot}66\ (\pm\ 0{\cdot}21) + 0{\cdot}71 \ln(\text{SLA})\ (\pm\ 0{\cdot}07) + 0{\cdot}79 \ln(N_M)\ (\pm\ 0{\cdot}10)$$

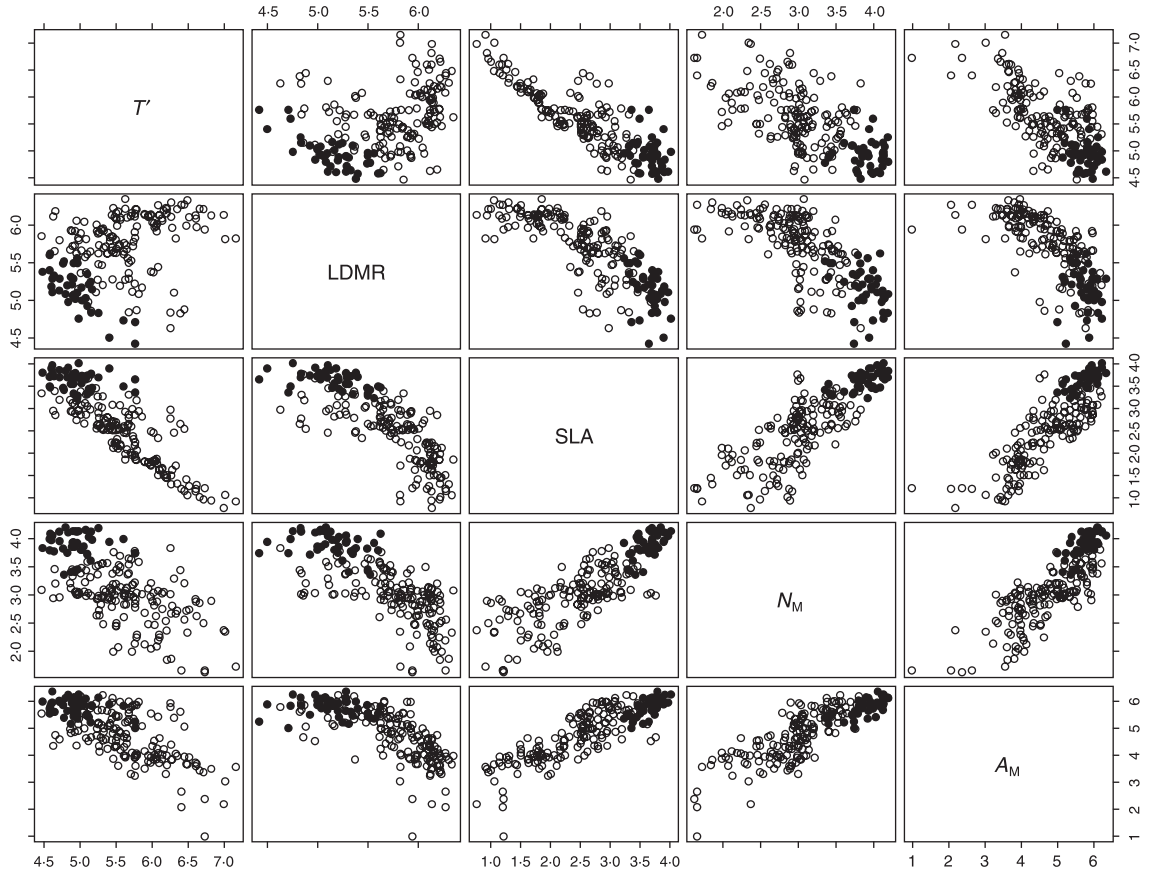

Fig. 2. Scatterplot matrix of the measured variables for leaf-level (open circles) and whole-plant (filled circles) data. Specific leaf area (SLA, $m^2\ kg^{-1}$); leaf thickness (T, μm); leaf dry matter ratio (LDMR, mg dry mass g^{-1} fresh mass); leaf nitrogen mass fraction (N_M, mmol N g^{-1}); and net photosynthetic rate (A_M, nmol $CO_2\ g^{-1}\ s^{-1}$) from species with widely differing leaf morphologies, including both herbaceous and woody species. All variables are ln-transformed.

$$\text{plants} = \ln(A_M) = 0{\cdot}11\ (\pm 0{\cdot}21) + 0{\cdot}71\ \ln(\text{SLA}) \\ (\pm 0{\cdot}07) + 0{\cdot}79\ \ln(N_M)\ (\pm 0{\cdot}10) \qquad \text{eqn 6}$$

To compare our results with those reported by Reich *et al*. (1999), we present Fig. 3 in which their data are superimposed on ours and our prediction equation for individual leaves.

Finally, we regressed ln(A) on ln(T'), ln(LDMR), ln(N_M) and a dummy variable representing the type of data (leaf level or whole plant) and evaluated significance using type III sums of squares. The slopes associated with all three predictor variables were highly significant ($P < 0{\cdot}001$). Only the slope of ln(LDMR) differed between the two types of data ($P < 0{\cdot}001$), with that for whole plants being more negative (–2·05 *vs* –1·34). There was also a significant three-way interaction between ln(LDMR), ln(N_M) and ln(T') ($P < 0{\cdot}02$). These interactions, although real, changed the predicted values only marginally over the measured range of the data. We therefore report the simpler regression (r2 = 0·80, residual SE = 0·43) ignoring all interactions:

$$\text{leaves} = \ln(A_M) = 10{\cdot}20\ (\pm 1{\cdot}00) + 0{\cdot}77\ \ln(N_M)\ (\pm 0{\cdot}10) \\ - 0{\cdot}61\ \ln(T')\ (\pm 0{\cdot}07) - 0{\cdot}81\ \ln(\text{LDMR})\ (\pm 0{\cdot}10)$$

$$\text{plants} = \ln(A_M) = 9{\cdot}91\ (\pm 1{\cdot}00) + 0{\cdot}77\ \ln(N_M)\ (\pm 0{\cdot}10) \\ - 0{\cdot}61\ \ln(T')\ (\pm 0{\cdot}07) - 0{\cdot}81\ \ln(\text{LDMR}) \\ (\pm 0{\cdot}10) \qquad \text{eqn 7}$$

STRUCTURAL EQUATION MODELS

The structural equation model derived from the original mechanistic model of Evans and Poorter (Fig. 1a) provided a very poor fit to the empirical data ($\chi^2 = 69{\cdot}81$, 5 df, $P < 5 \times 10^{-6}$). This was true although every individual hypothesized cause–effect link in the model ($T \rightarrow$ SLA, $C_M \rightarrow$ SLA, SLA $\rightarrow A_M$, $N_M \rightarrow A_M$) was significantly different from zero and provided good predictive ability; the r^2 values for ln(SLA), ln(A_M), ln(LDMC) and ln(T') in this rejected model were 0·955, 0·689, 0·996 and 0·889, respectively. The lack of fit came from the incorrect predictions of partial correlation (i.e. the assumed indirect links) between the variables suggested by the overall structure of the model. However, the modified version of the Evans–Poorter model (Fig. 1b) provided a good fit to the data ($\chi^2 = 1{\cdot}55$, 3 df, $P = 0{\cdot}67$). Each free path coefficient was significantly different from zero, and each was of the correct sign. This fitted model is shown in Fig. 4(a). Figure 4(b) shows an alternative model that provides a

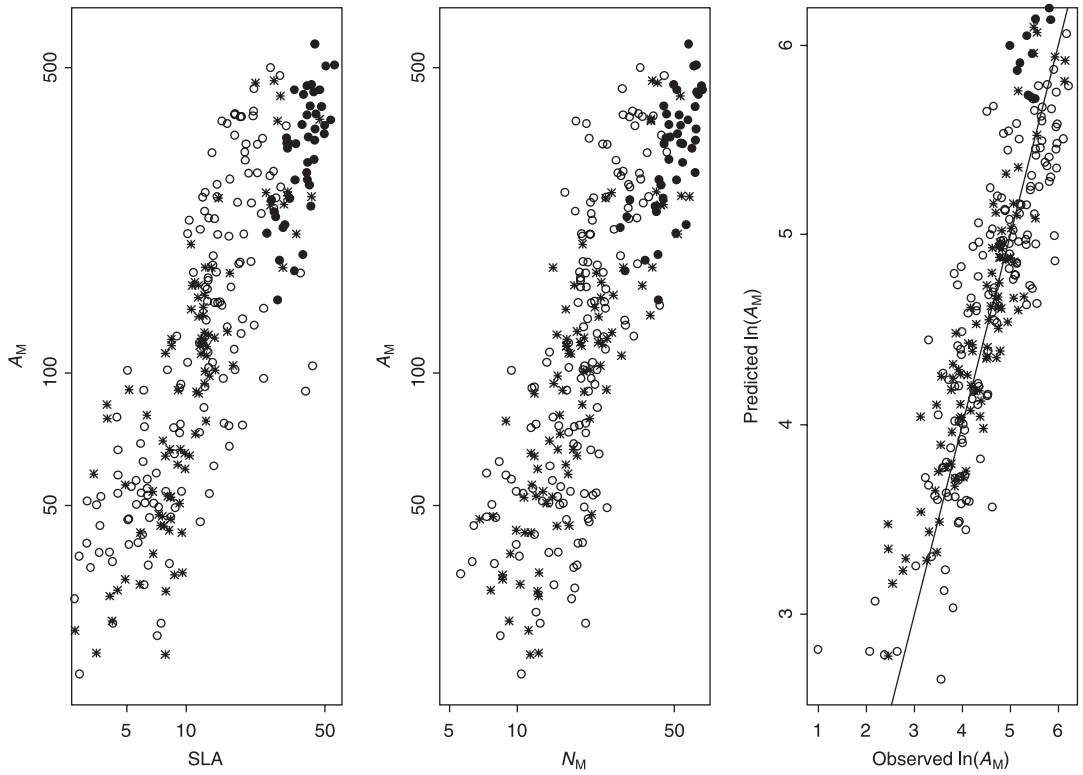

Fig. 3. Scatterplots of net photosynthetic rate (A_M, nmol CO_2 g^{-1} s^{-1}) *vs* SLA (m^2 kg^{-1}) and leaf nitrogen mass fraction (N_M, mmol g^{-1}) for whole-plant (solid circles) and leaf-level data (open circles) from this paper and from Reich *et al.* (1999) (stars). The last graph plots observed net photosynthetic rates against predicted values using the regression equation from our leaf data only.

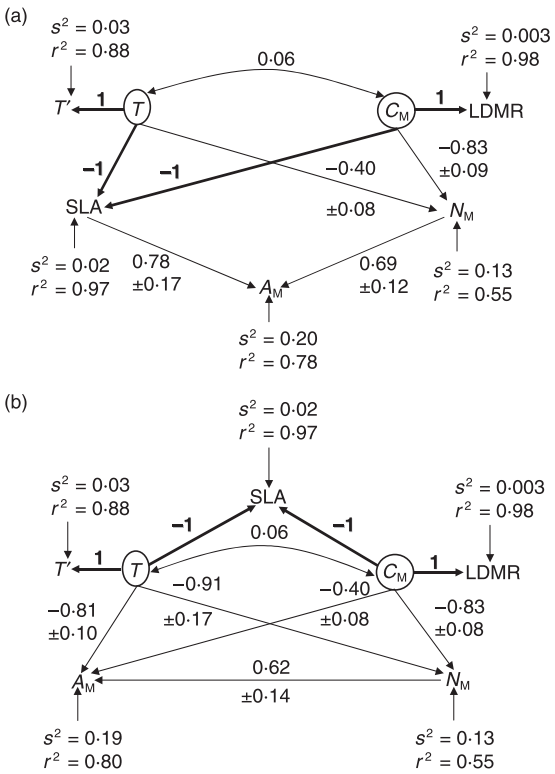

Fig. 4. Two alternative path models that fit the leaf-level data. Maximum likelihood estimates of the path coefficients are given along with standard errors. Thick lines and values without standard errors are fixed. Also shown are residual variances (s^2) and explained variation (r^2) of each endogenous variable. Variables enclosed in circles are latent.

slightly better fit ($\chi^2 = 0{\cdot}16$, 2 df, $P = 0{\cdot}92$), which was developed using an exploratory method (Shipley 1997). Although apparently different, this second model is actually very similar to that in Fig. 4(a). This is because, given the extremely strong correlations between T, T', C_M, LDMR and SLA, the direct and indirect paths linking these variables to A_M and N_M are also similar. Finally, we tested another model, similar to that in Fig. 4(a) but in which N_M is directly caused only by SLA rather than by T and C_M, that is, T and C_M are indirect causes of N_M. This model was rejected ($\chi^2 = 12{\cdot}11$, 4 df, $P = 0{\cdot}02$). Thus SLA is only spuriously correlated to N_M because SLA and N_M are caused by T and C_M, and each of T and C_M have effects on A_M that are independent of their effects on SLA.

We next tested the whole-plant data with the same two models as in Fig. 4. Both models were clearly rejected ($P < 10^{-4}$). However, examination of the residuals revealed that the lack of fit for the model in Fig. 1(b) was due to the requirement that the estimates of leaf thickness (T') for these whole-plant data be an unbiased estimate of the actual average leaf thickness (T); this requirement was imposed by fixing the path coefficient to unity between T and T' (cf. Figure 1b). Because T' in the whole-plant model was obtained from SLA and LDMR, rather than being directly measured, and as this could have resulted in a systematic deviation from a 1 : 1 relationship between T and T', we allowed the $T \rightarrow T'$ slope to be estimated from the data rather than being imposed. The fits of the models were

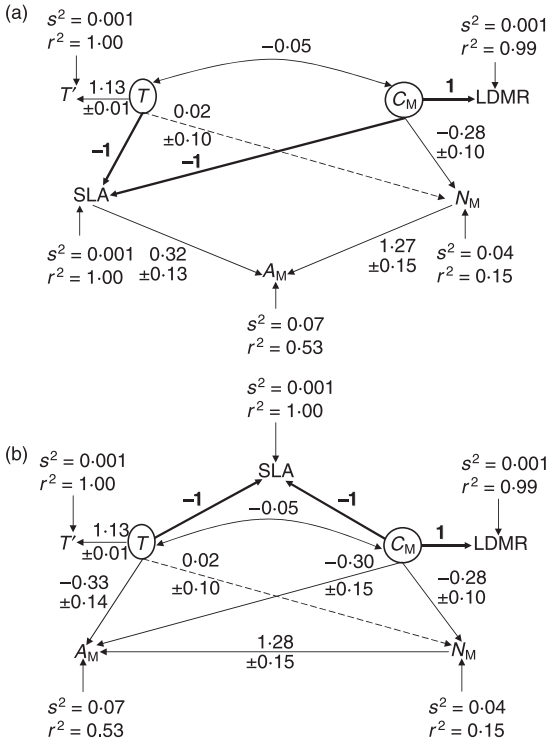

Fig. 5. The same two alternative path models as in Fig. 4 that fit the whole-plant data. Dashed lines represent paths whose coefficient are not significantly different from zero. See Fig. 4 for more information.

substantially improved (Fig. 5a: $\chi^2 = 4{\cdot}55$, 2 df, $P = 0{\cdot}10$; Fig. 5b: $\chi^2 = 4{\cdot}31$, 1 df, $P = 0{\cdot}04$). The path coefficient from the true leaf thickness to the estimated thickness was 1·13 (SE 0·01), showing that the thickness of thinner leaves was systematically (but only slightly) underestimated relative to thicker leaves. Furthermore, there were two data points that were clear outliers and from the same species (*Plantago major*, reported by Dijkstra & Lambers 1989) that, together, accounted for 46% of the parameter variance and whose leaf thickness values were approximately three times larger than the others. If these two data points are removed, the two models provide an acceptable fit to the data (Fig. 5a: $\chi^2 = 3{\cdot}44$, 2 df, $P = 0{\cdot}18$; Fig. 5b: $\chi^2 = 3{\cdot}368$, 1 df, $P = 0{\cdot}07$). The path coefficient from leaf thickness to leaf N content was small and not significantly different from zero in these whole-plant data.

SIMULATION MODELS

Ideally, one would obtain the parameter values of equation 3 for each species in the data set. It is because this is not possible in practice that such mechanistic simulation models are so difficult to apply to comparative ecology. Instead, we apply the model parameters from Evans & Poorter (2001) at an irradiance of 1000 μmol m^{-2} s^{-1}, as photosynthesis would be close to light saturation at this level (Table 1), and we compare observed and predicted relative values of A_M, (A_M as a proportion of the maximal A_M observed or predicted). Figure 6(a) (open circles) plots the observed relative values of A_M and SLA ($r = 0{\cdot}66$, $P < 0{\cdot}001$). The quantiles of N_M in the empirical field data were: minimum = 0·36, 5% = 0·52, 25% = 1·03, 50% = 1·41, 75% = 1·75, 95% = 2·58, maximum = 3·29 mmol g^{-1}. The seven solid non-linear lines in each of the three graphs in Fig. 6 show the model predictions relating A_M and SLA at these seven N mass fractions. The relative values of A_M that are predicted by the original Evans–Poorter model, given only SLA and N_M, are shown in Fig. 6(b) (filled circles). These predicted values are close to the observed values, although the predicted values tend to overestimate A_M for a given SLA. At each N_M, A_M increases with SLA up to a maximum, after which A_M decreases. As expected, leaves with a higher N_M are predicted to have a higher A_M at a given value of SLA. However, the value of SLA that maximizes A_M is predicted to increase linearly with increasing N_M even though irradiance is constant: the equation describing this optimal combination of SLA and N_M is SLA = $0{\cdot}43 + 7{\cdot}68N_M$. The empirical regression of SLA on N_M (thin line) is SLA = $1{\cdot}86 + 7{\cdot}49N_M$ ($r = 0{\cdot}59$, $P < 0{\cdot}001$). Neither the slope nor the intercept of this regression is significantly different from that of the optimal line: $t = 1{\cdot}09$, $P = 0{\cdot}28$ (intercept); $t = -0{\cdot}23$, $P = 0{\cdot}82$ (slope). Figure 7(a) shows the empirical relationship between SLA and N_M as well as this predicted optimal relationship. On average, SLA and N_M covary in these leaves around those values predicted by the original Evans–Poorter model to maximize A_M, although there is substantial residual variation around these optima. Furthermore, the predicted optimal relative A_M–SLA relationship closely follows the limiting values observed in the empirical data (Fig. 6, left).

The modified version of the Evans–Poorter model removes N_M and SLA as independent forcing variables and replaces them with T and C_M. SLA is calculated from $1/(TC_M)$. N_M is predicted from the structural equation model (remembering that the structural equation must pass through the grand means of SLA, T and C_M) as $N_M = 6{\cdot}25/T^{0{\cdot}40}C_M^{0{\cdot}83}$; in other words, this modified model requires only T and C_M and does not require empirical information about N_M. Note that, for a fixed SLA, a compensatory increase in C_M and decrease in T reduces N_M. Figure 6(b) (solid circles) shows the model output. Despite the facts that this modified model predicts N_M rather than having N_M provided as independent data, and that the model did not constrain these predicted N_M values to follow those that would maximize A_M, the predicted relative values of A_M do follow the maximal values predicted given only T and C_M. Figure 8(a) shows the relationship between the observed and predicted values. The correlation coefficient is 0·74, but there are three species (filled circles) whose predicted values of relative A_M are much higher that actually observed (two plants of *Acer saccharum* and one of *Acer platinoides* from Kloeppel & Abrams 1995) (Fig. 7a). The N_M predicted for these species (and therefore the A_M) is higher than is observed,

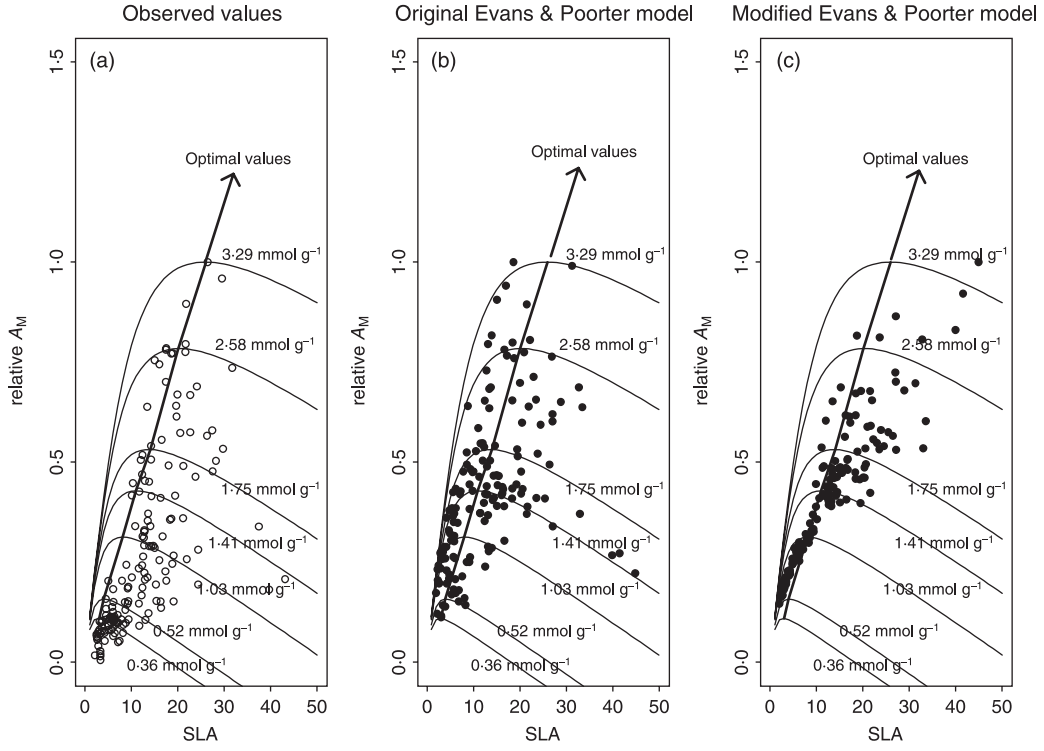

Fig. 6. (a) Observed values of net photosynthetic rate (A_M nmol g^{-1} s^{-1}) relative to its maximum value *vs* SLA (m^2 kg^{-1}) for leaf-level data. The solid, non-linear curves are predicted values of the original Evans–Poorter at different leaf nitrogen mass fraction. Arrow, combinations of A_M and SLA that maximize A_M for a given N_M according to the Evans–Poorter model. (b) Predicted values of net photosynthetic rate relative to the maximum value *vs* SLA for leaf-level data given by the Evans–Poorter model. (c) Predicted values of net photosynthetic rate (A_M) relative to the maximum value *vs* SLA for leaf-level data given by the modified Evans–Poorter model.

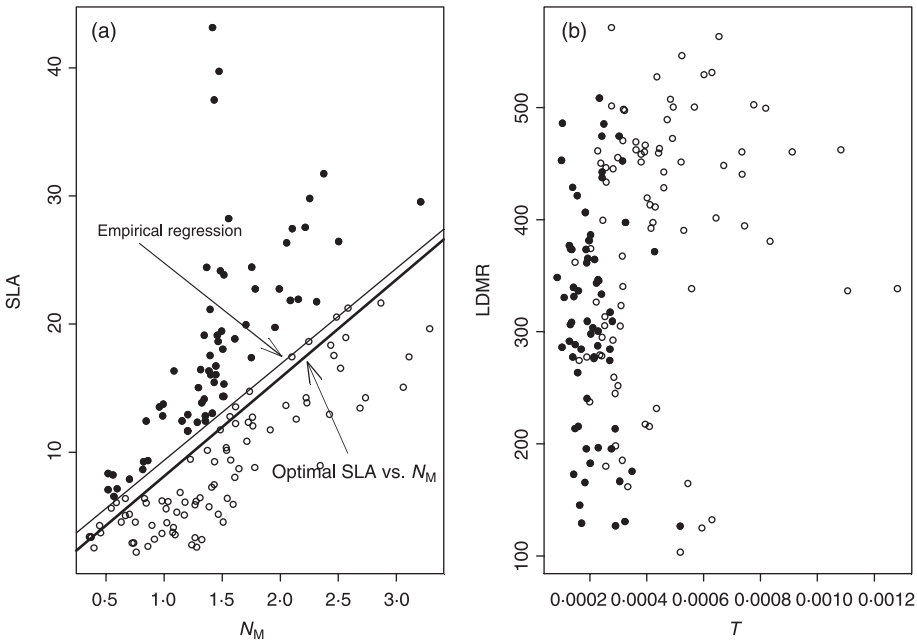

Fig. 7. (a) Observed values of leaf nitrogen mass fraction (N_M, mmol g^{-1}) and SLA (m^2 kg^{-1}). Also shown is the regression line (SLA = 1·86 + 7·49N_M, r = 0·59, P < 0·001) and the SLA–N_M combinations that are predicted to maximize A_M in the Evans–Poorter model (SLA = 0·43 + 7·68N_M). (b) Leaf dry matter ratio (mg dry mass g^{-1} fresh mass) *vs* leaf thickness. Filled circles are observations for which N_M was less than expected given SLA.

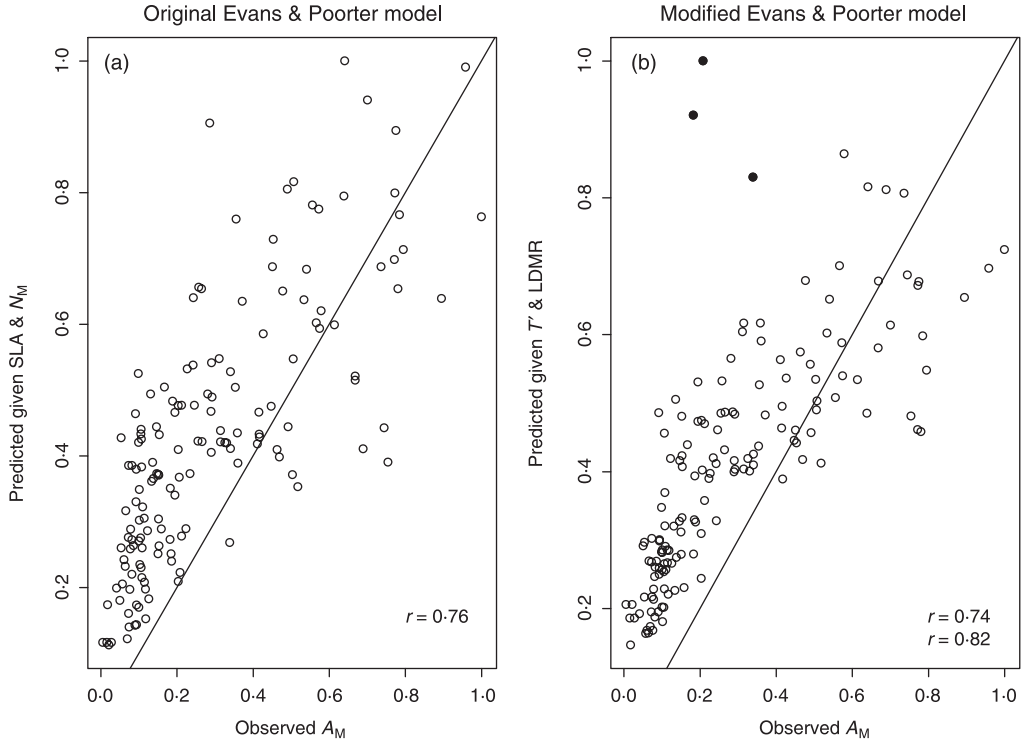

Fig. 8. (a) Observed and predicted values of net photosynthetic rate (A_M, nmol g^{-1} s^{-1}) relative to the maximal values of the original Evans–Poorter model; $r = 0{\cdot}76$. Also shown is the 1 : 1 line. (b) The same two variables, using the predicted values of the modified Evans–Poorter model; $r = 0{\cdot}74$. Three outliers are shown by solid circles; if these are removed, $r = 0{\cdot}82$.

as the modified model predicts N_M from T and C_M. If these three outliers are removed, then the correlation coefficient increases to 0·82.

Discussion

For most plants the primary function of leaves is to fix C. Although many different morphological and physiological attributes must interact to determine net C fixation within a given environmental context, there are certain combinations of traits that are either physically impossible, or that lead to such suboptimal returns on C fixation that those combinations have been removed by natural selection. Presumably, the empirical relationships between A_M, N_M and SLA derive from such physical and evolutionary constraints. The objective of this paper was to develop a mathematical model that can link these empirical interspecific patterns to underlying mechanistic processes, and then to explore the consequences of such trade-offs for comparative ecology.

EMPIRICAL RELATIONSHIPS

Leaf-level photosynthetic rate was correlated with SLA at an interspecific level, and the correlation was strengthened when combined with leaf N_M. Such patterns have been reported already in the literature, and our results confirm these trends. In particular, Fig. 3 shows a good quantitative concordance between our leaf-level relationships and those previously reported (Reich *et al*. 1999), and emphasizes the generality and importance of this empirical relationship. The relationship is also robust to experimental manipulation. Meziane & Shipley (2001), in a controlled-environment study of 22 herbaceous species, found that at high irradiance (1100 μmol m^{-2} s^{-1}) the changes induced in A_M by changing the nutrient supply followed those predicted by the multiple regression of Reich *et al*. (1999). Reducing the irradiance to 200 μmol m^{-2} s^{-1} changed the intercept of the mean A_M but not the slope of the relationship.

It is surprising that our whole-plant data generally fall within the scatter of the leaf-level data, which would allow one to scale up from single leaves to whole plants. This result must remain tentative, for several reasons. First, all the whole-plant data came from single herbaceous plants grown in hydroponic solution, at irradiance levels below those found in the leaf-level data (Table 2) and with much less self-shading than is typical in nature. Second, they came from a biased subset of species having leaves that were thinner, less dense (as estimated by LDMC), and having more leaf N per dry mass than most of the leaf-level data. Many of the whole-plant data come from grasses, and the relationship between leaf thickness and leaf tissue density differs from that in dicots (Pyankov *et al*. 1999).

$\ln(A_M)$ is also correlated with ln(LDMR) and $\ln(T')$, and these two variables together have the same predictive ability as ln(SLA). Whereas projected surface area is difficult to measure and interpret in species lacking typical laminar leaves, we note that LDMR and T' can

be applied to any photosynthetic organ. It would be interesting to determine if the regression equation holds for species lacking laminar leaves.

LINKING EMPIRICAL AND MECHANISTIC MODELS

The regression equations discussed above are important because they are applicable to the leaves of a wide range of plant species in the field when growing in full light. Why do these empirical relationships recur? Presumably, they are generated by some basic physical or functional constraints on leaf form and function, but the regression equations themselves cannot identify these constraints and certainly cannot be used to argue for or against any particular mechanistic explanation. A mechanistic explanation is proposed in the simulation model of Evans & Poorter (2001). This explanation is explicit in the cause–effect links between the leaf attributes included in the mechanistic model. How can one map this explanation of the mechanistic model to the more general empirical patterns described by regression equations? Once the mapping has been made, how can one empirically test the assumed explanation, as represented by the network of direct and indirect relationships?

To produce such a link, we first converted the Evans–Poorter model into a directed acyclic graph and then used the graph theoretical operation of d-separation to predict how it must be modified when some of its variables become latent, that is, unmeasured but still imposing constraints on the patterns of correlation between the remaining variables. Given the new reduced graph, we then tested the predicted patterns of direct and indirect correlation that are suggested by the graph (and therefore also by the original Evans–Poorter model) using structural equation modelling. The model associated with the original Evans–Poorter model was rejected by the data, and this was due to the assumption that N_M is causally independent of SLA, T and C_M. Another model, in which there was a direct effect SLA $\rightarrow N_M$, and in which both T and C_M were only indirect causes of N_M through their effects on SLA, was also rejected by the data. Besides this statistical reason for rejecting a model with SLA $\rightarrow N_M$, we can think of no biological mechanism to justify such a link. However, as argued in the Introduction, there are biological reasons to expect that changes in leaf thickness and tissue concentration (T, C_M) would induce changes in leaf N_M. The directed graph, derived from the modified Evans–Poorter model, which incorporates these effects, provided a good fit to the data. Thus the empirical correlation between SLA and N_M is spurious because both SLA and N_M decrease with increasing values of T and C_M.

Although this modified Evans–Poorter model successfully predicts the patterns of direct and indirect correlation between the measured variables, and although its predicted values of A_M agree closely (at least on a relative scale) with the observed values, there was an even more surprising fit between model and data. The original Evans–Poorter model predicted that, to maximize A_M, a leaf must co-ordinate its SLA and N_M such that SLA = $0{\cdot}43 + 7{\cdot}68N_M$. This prediction was a consequence of the model and was not based on any empirical constraint, yet the empirical regression of SLA on N_M agreed closely and showed no significant deviation from the theoretical relationship. As the structural equation model based on the modified Evans–Poorter model provided the predicted relationship between N_M and its two direct causes, T and C_M (and also its two indirect indicators, T' and LDMR), we parameterized the modified Evans–Poorter model using this predicted relationship. The resulting model predicted A_M just as well as the original Evans–Poorter model (even better if we exclude three clear outliers), although the predictions of this modified model were obtained using only T' and LDMR. Significantly, the predicted values of SLA and A_M followed those predicted to optimize A_M. It would be interesting to compare this predicted relationship between SLA and N_M with the notion of the critical N fraction in crop modelling (Lemaire & Millard 1999).

FROM MECHANISTIC PATHS TO STRUCTURAL PATHS TO EMPIRICAL REGRESSIONS

We can directly map the paths in the path model (Fig. 4a) to the paths of the modified Evans–Poorter model (cf. Figure 1b). The $T \rightarrow$ SLA $\rightarrow A_M$ path in the path model is derived from the sum of $T \rightarrow$ SLA $\rightarrow N_A \rightarrow \alpha \rightarrow A_A \rightarrow A_M + T \rightarrow$ SLA $\rightarrow N_A \rightarrow J_{max} \rightarrow A_A \rightarrow A_M$ paths of the modified Evans–Poorter mechanistic model. These two paths in the mechanistic model represent the effect that changes in leaf thickness would have on A_M if N_M was held constant. This occurs solely by changing the surface : dry mass ratio of the leaf. Changing this ratio changes (i) the proportion of incident light absorbed by the leaf by changing the chlorophyll content per unit leaf area; and (ii) the electron transport capacity by changing the allocation of N per unit leaf area between thylakoid N, soluble protein N and chlorophyll (see equation 10 of Evans & Poorter 2001). The $C_M \rightarrow$ SLA $\rightarrow A_M$ path in the path model is interpreted in the same way relative to the mechanistic model.

The $T \rightarrow N_M \rightarrow A_M$ and $C_M \rightarrow N_M \rightarrow A_M$ paths in the path model have a different interpretation. The $T \rightarrow N_M \rightarrow A_M$ path is derived from the $T \rightarrow N_M \rightarrow N_A \rightarrow \alpha \rightarrow A_A \rightarrow A_M + T \rightarrow N_M \rightarrow N_A \rightarrow J_{max} \rightarrow A_A \rightarrow A_M$ paths of the modified Evans–Poorter model, and describes how changes in leaf thickness affect the amount of soluble leaf N per unit dry mass for a leaf with a constant SLA, which then cascades throughout the rest of the path. In other words, different trade-offs between T and C_M for a given SLA will have different consequences for N_M and therefore A_M. A similar interpretation is obtained for the $C_M \rightarrow N_M \rightarrow A_M$

path. Finally, there is the SLA $\rightarrow A_A \rightarrow A_M$ path that converts the area-based measure to the mass-based measure. Note that the first step in these paths ($T \rightarrow N_M$ and $C_M \rightarrow N_M$) is not derived from any mechanistic link in the original Evans–Poorter model; indeed, these paths are absent from the original model. It will therefore be important to better explicate this path in mechanistic terms. We have explained in the Introduction how variation in mesophyll cell sizes (surface : volume ratios) and the proportions of fibres and non-structural carbohydrates could all lead to such a path, but this explanation must remain speculative until these are measured and explicitly included in a path model. However, each of these hypotheses can be formalized in an extended version of the path model, and tested.

ECOLOGICAL AND EVOLUTIONARY CONSEQUENCES

Plants adjust their SLA to the ambient light conditions under which the leaves develop. Decreased light increases SLA (Hanson 1917; Abrams & Kubiske 1990), and this also holds in interspecific comparisons (Smith *et al*. 1998). Indeed, Evans & Poorter (2001) developed their original model to explore why this should occur. However, little is known about the relationship between SLA and nutrient availability. Experimental studies suggest that SLA decreases with decreasing nutrient supply (Hirose *et al*. 1988; van Arendonk *et al*. 1997, Meziane & Shipley 1999). Witkowski *et al*. (1992) reported that leaves of two Australian tree species growing in dryer and more nutrient-poor soils also had a lower SLA due to thicker leaves with more dense tissues. Certainly, sclerophylly is associated with nutrient-poor conditions independent of water supply, as such leaves are typical of plants growing in acidic, nutrient-poor bogs (Pensa & Sellin 2002; Campbell & Rochefort 2003; Niinemets & Kull 2003; Burns 2004). The Evans–Poorter model provides an explanation for this trend: to maximize A_M the leaf must co-ordinate its SLA and N_M to balance the amount of organic leaf N per mass with the surface : dry mass ratio which determines the N content per unit area. Surprisingly, the empirical relationship between SLA and N_M follows the theoretical relationship that maximizes A_M to within the statistical precision available to us. In doing so, leaves must simultaneously modify T and C_M, as both determine SLA and N_M; there is, of course, substantial variation in N_M that is not related to these morphological attributes, but that contributes to variation in A_M. Leaves are free to vary this part of N_M independently of T and C_M, and this means that the SLA–N_M constraint is not absolute. As a consequence, there is also residual variation around the predicted optimal values of relative A_M in the mechanistic models.

What might be the origin of these deviations from optimality? It seems unlikely that leaves have actually evolved to maximize instantaneous C fixation. Rather, fitness should be more closely related to net C fixation over the lifetime of the leaf. Leaf life span is negatively correlated with SLA (Reich *et al*. 1998). The degree to which leaf thickness *vs* leaf tissue concentration determines leaf life span has not been studied in detail, but Wright & Westoby (2002) report a better correlation for T than C_M. Looking at Fig. 6, we see that when a species has a suboptimal A_M for a given SLA, it also has a suboptimal N_M for that SLA. This results in a non-linear relationship, as species with higher SLA are apparently more suboptimal. This occurs, according to the model, because the leaf has a relatively higher C_M and a relatively lower T for that value of SLA. Figure 7(b) shows that those species with a lower than expected N_M for a given SLA are those that are thinner but with denser leaves. The inclusion of leaf life span and lifetime A_M in the model might explain some of the residual deviation. If so, then combinations of C_M and T that are suboptimal with respect to simultaneous A_M might still maximize leaf lifetime A_M. These hypotheses are testable using our approach and can be cast in mechanical terms (Niklas 1992). Only the data are missing.

Acknowledgements

This research was financially supported by the Natural Sciences and Engineering Research Council (NSERC) of Canada.

References

Abrams, M.D. & Kubiske, M.E. (1990) Leaf structural characteristics of 31 hardwood and conifer tree species in central Wisconsin. Influence of light regime and shade-tolerance rank. *Forest Ecology Management* **31**, 245–253.

Abrams, M.D. & Mostoller, S.A. (1995) Gas exchange, leaf structure and nitrogen in contrasting successional tree species growing in open and understory sites during a drought. *Tree Physiology* **15**, 361–370.

van Arendonk, J.J.C.M., Niemann, G.J., Boon, J.J. & Lambers, H. (1997) Effects of nitrogen supply on the anatomy and chemical composition of leaves of four grass species belonging to the genus *Poa*, as determined by image-processing analysis and pyrolysis-mass spectrometry. *Plant, Cell & Environment* **20**, 881–897.

Atkin, O.K., Botman, B. & Lambers, H. (1996) The causes of inherently slow growth in alpine plants: an analysis based on the underlying carbon economies of alpine and lowland *Poa* species. *Functional Ecology* **10**, 698–707.

Bentler, P.M. (1995) *EQS Structural Equations Program Manual, Version 3·0*. BMDP Statistical Software, Los Angeles, CA, USA.

Burns, K.C. (2004) Patterns in specific leaf area and the structure of a temperate heath community. *Diversity and Distributions* **10**, 105–112.

Campbell, D.R. & Rochefort, L. (2003) Germination and seedling growth of bog plants in relation to the recolonization of milled peatlands. *Plant Ecology* **169**, 71–84.

Chazdon, R.L. & Kaufmann, S. (1993) Plasticity of leaf anatomy of two rain forest shrubs in relation to photosynthetic light acclimation. *Functional Ecology* **7**, 385–394.

Den Dubbelden, K.C. (1994) *Growth and Allocation Patterns in Herbaceous Climbing Plants*. Utrecht University, Utrecht, the Netherlands.

Dijkstra, P. & Lambers, H. (1989) Analysis of specific leaf area and photosynthesis of two inbred lines of *Plantago major* differing in relative growth rate. *New Phytologist* **113**, 283–290.

Evans, J.R. & Poorter, H. (2001) Photosynthetic acclimation of plants to growth irradiance: the relative importance of specific leaf area and nitrogen partitioning in maximizing carbon gain. *Plant, Cell & Environment* **24**, 755–767.

Farquhar, G.D. & Von Caemmerer, S. (1982) Modelling of photosynthetic response to environmental conditions. *Encyclopedia of Plant Physiology* (ed. H. Ziegler), pp. 549–587. Springer-Verlag, Berlin.

Field, C. & Mooney, H.A. (1986) The photosynthesis–nitrogen relationship in wild plants. *On the Economy of Plant Form and Function* (ed. T.J. Givnish), pp. 25–55. Cambridge University Press, Cambridge, UK.

Garnier, E. & Laurent, G. (1994) Leaf anatomy, specific mass and water content in congeneric annual and perennial species. *New Phytologist* **128**, 725–736.

Garnier, E., Salager, J.L., Laurent, G. & Sonie, L. (1999) Relationships between photosynthesis, nitrogen and leaf structure in 14 grass species and their dependence on the basis of expression. *New Phytologist* **143**, 119–129.

Hanson, H.C. (1917) Leaf-structure as related to environment. *American Journal of Botany* **4**, 533–560.

Hirose, T., Freijsen, A.H.J. & Lambers, H. (1988) Modelling of the responses to nitrogen availability of two *Plantago* species grown at a range of exponential nutrient addition rates. *Plant, Cell & Environment* **11**, 827–834.

Kloeppel, B.D. & Abrams, M.D. (1995) Ecophysiological attributes of the native *Acer saccharum* and the exotic *Acer platanoides* in urban oak forests in Pennsylvania, USA. *Tree Physiology* **15**, 739–746.

Körner, C. & Diemer, M. (1987) *In situ* photosynthetic responses to light, temperature and carbon dioxide in herbaceous plants from low and high altitude. *Functional Ecology* **1**, 179–194.

Lemaire, G. & Millard, P. (1999) An ecophysiological approach to modelling resource fluxes in competing plants. *Journal of Experimental Botany* **50**, 15–28.

Meziane, D. & Shipley, B. (1999) Interacting determinants of specific leaf area in 22 herbaceous species: effects of irradiance and nutrient availability. *Plant, Cell & Environment* **22**, 447–459.

Meziane, D. & Shipley, B. (2001) Direct and indirect relationships between specific leaf area, leaf nitrogen and leaf gas exchange. Effects of irradiance and nutrient supply. *Annals of Botany* **88**, 915–927.

Niinemets, U. & Kull, K. (2003) Leaf structure vs. nutrient relationships vary with soil conditions in temperate shrubs and trees. *Acta Oecologica* **24**, 209–219.

Niklas, K.J. (1992) *Plant Biomechanics. An Engineering Approach to Plant Form and Function*. University of Chicago Press, Chicago, IL, USA.

Pammenter, N.W., Dreggan, M. & Smith, V.R. (1986) Physiological and anatomical aspects of photosynthesis of two *Agrostis* species at a sub-Antarctic island. *New Phytologist* **102**, 143–160.

Pearl, J. (1995) Causal diagrams for empirical research. *Biometrika* **82**, 669–709.

Pearl, J. (2000) *Causality*. Cambridge University Press, Cambridge, UK.

Pensa, M. & Sellin, A. (2002) Needle longevity of Scots pine in relation to foliar nitrogen content, specific leaf area and shoot growth in different forest types. *Canadian Journal of Forest Research* **32**, 1225–1231.

Poorter, H. (1990) Interspecific variation in relative growth rate: on ecological causes and physiological consequences. *Causes and Consequences of Variation in Growth Rate and Productivity in Higher Plants* (ed. T.L. Pons), pp. 45–68. SPB Academic Publishing, The Hague.

Poorter, H. & Remkes, C. (1990) Leaf area ratio and net assimilation rate of 24 species differing in relative growth rate. *Oecologia* **83**, 553–559.

Poorter, H. & Villar, R. (1997) The fate of acquired carbon in plants: chemical composition and construction costs. *Plant Resource Allocation* (ed. J. Grace), pp. 39–72. Academic Press, San Diego, CA, USA.

Pyankov, V., Kondratchuk, A. & Shipley, B. (1999) Leaf structure and specific leaf mass: the alpine desert plants of the Eastern Pamirs (Tadjikistan). *New Phytologist* **143**, 131–142.

Reich, P.B., Walters, M.B. & Ellsworth, D.S. (1997) From tropics to tundra: global convergence in plant functioning. *Proceedings of the National Academy of Sciences, USA* **94**, 13730–13734.

Reich, P., Walters, M.B., Ellsworth, D.S. *et al.* (1998) Relationships of leaf dark respiration to leaf nitrogen, specific leaf area and leaf life-span: a test across biomes and functional groups. *Oecologia* **114**, 471–482.

Reich, P.B., Ellsworth, D.S., Walters, M.B. *et al.* (1999) Generality of leaf trait relationships: a test across six biomes. *Ecology* **80**, 1955–1969.

Van Rijn, C. (2001) A physiological and genetic analysis of growth characteristics in *Hordeum spontaneum*. PhD thesis, Utrecht University, Utrecht, the Netherlands.

Roderick, M.L., Berry, S.L., Noble, I.R. & Farquhar, G.D. (1999a) A theoretical approach to linking the composition and morphology with the function of leaves. *Functional Ecology* **13**, 683–695.

Roderick, M.L., Berry, S.L., Saunders, A.R. & Noble, I.R. (1999b) On the relationship between the composition, morphology and function of leaves. *Functional Ecology* **13**, 696–710.

Shipley, B. (1997) Exploratory path analysis with applications in ecology and evolution. *American Naturalist* **149**, 1113–1138.

Shipley, B. (2000a) *Cause and Correlation in Biology: A User's Guide to Path Analysis, Structural Equations, and Causal Inference*. Oxford University Press, Oxford, UK.

Shipley, B. (2000b) A new inferential test for path models based on directed acyclic graphs. *Structural Equation Modeling* **7**, 206–218.

Shipley, B. (2003) Testing recursive path models with correlated errors using d-separation. *Structural Equation Modeling* **10**, 214–221.

Shipley, B. & Lechowicz, M.J. (2000) The functional coordination of leaf morphology, nitrogen concentration, and gas exchange in 40 wetland species. *Ecoscience* **7**, 183–194.

Shipley, B. & Vu, T.-T. (2002) Dry matter content as a measure of dry matter concentration in plants and their parts. *New Phytologist* **153**, 359–364.

Smith, W.K., Bell, D.T. & Shepherd, K.A. (1998) Associations between leaf structure, orientation, and sunlight exposure in five Western Australian communities. *American Journal of Botany* **85**, 56–63.

Spirtes, P., Glymour, C. & Scheines, R. (1993) *Causation, Prediction, and Search*. Springer-Verlag, New York, USA.

Spirtes, P., Glymour, C. & Scheines, R. (2000) *Causation, Prediction, and Search*, 2nd edn. MIT Press, Cambridge, MA, USA.

SPLUS (1999) *s-plus 2000 User's Guide*. MathSoft, Seattle, WA, USA.

Van Arendonk, J.J.C.M. & Poorter, H. (1994) The chemical composition and anatomical structure of leaves of grass species differing in relative growth rate. *Plant, Cell & Environment* **17**, 963–970.

Van den Boogaard, R., Goubitz, S., Veneklaas, E.J. & Lambers, H. (1996) Carbon and nitrogen economy of four *Triticum aestivum* cultivars differing in relative growth rate and water use efficiency. *Plant, Cell & Environment* **19**, 998–1004.

Van der Werf, A., Van Nuenen, M.A.J., V. & Lambers, H. (1993) Contribution of physiological and morphological plant traits to a species' competitive ability at high and low nitrogen supply. A hypothesis for inherently fast- and slow-growing monocotyledonous species. *Oecologia* **94**, 434–440.

Van Rijn, C.P.E., Heersche, I., Van Berkel, Y.E.M., Nevo, E., Lambers, H. & Poorter, H. (2000) Growth characteristics in *Hordeum spontaneum* populations from different habitats. *New Phytologist* **146**, 471–481.

Von Caemmerer, S., Evans, J.R., Hudson, G.S. & Andrews, T.J. (1994) The kinetics of ribulose-1,5-biphosphate carboxylase/oxygenase *in vivo* inferred from measurements of photosynthesis in leaves of transgenic tobacco. *Planta* **195**, 88–97.

Witkowski, E.T.F., Lamont, B.B., Walton, C.S. & Radford, S. (1992) Leaf demography, sclerophylly and ecophysiology of two *Banksias* with contrasting leaf life spans. *Australian Journal of Botany* **40**, 849–862.

Woodward, F.I. (1986) Ecophysiological studies on the shrub *Vaccinium myrtillus* L. taken from a wide altitudinal range. *Oecologia* **70**, 580–586.

Wright, I.J. (2001) *Leaf Economics of Perennial Species from Sites Contrasted on Rainfall and Soil Nutrients*. Macquarie University, Sydney, Australia.

Wright, I.J. & Westoby, M. (2002) Leaves at low versus high rainfall: coordination of structure, lifespan and physiology. *New Phytologist* **155**, 403–416.

Zotz, G. & Winter, K. (1996) Diel patterns of CO_2 exchange in rainforest canopy plants. *Tropical Forest Plant Ecophysiology* (eds S.S. Mulkey, R.L. Chazdon & A.P. Smith), pp. 83–113. Chapman & Hall, New York.

Received 27 May 2004; revised 29 September 2004; accepted 1 November 2004